Ing. Paola Ranut
Prof. Enrico Nobile
Università degli Studi di Trieste
Dipartimento di Ingegneria e Architettura

Corso di Termofluidodinamica Computazionale

Multiphase flows:

characterization and numerical modeling

A.A. 2014-2015

Contents

1   Introduction

Multi-phase flows exist in many natural and technological systems. A multiphase flow can be defined as a flow in which there is the simultaneous presence of materials with different states or phases (i.e. gas, liquid or solid) or materials in the same state or phase but with different chemical properties (i.e. liquid-liquid systems such as oil droplets in water). In a multi-phase flow, one phase is regarded as continuous while the other(s) are dispersed within it. Moreover, each phase can be laminar or turbulent.

A multi-phase flow should not be confused with multi-component flow. In fact, while in a multicomponent flow the species are mixed at the molecular level, in a multi-phase flow the species are mixed at scales much larger than the molecular-length scales and can possess different velocity and temperature fields.

Multi-phase flows can be broadly classified as *disperse* flows and *separated* flows. The former consist of finite particles, drops or bubbles (the so-called disperse phase) distributed in the continuous phase, the latter include two or more continuous streams of different fluids separated by interfaces. The dispersed flows can be further categorized in homogeneous flows and bubbly flows. The homogeneous flow can be regarded as the asymptotic limit of a disperse flow, in which an infinite number of infinitesimally small particles are present. In this case, the relative motion between the phases can be neglected. On the contrary, in a bubbly flow even if the particles are much smaller than the pipe dimensions, the relative motion between the phases is significant.

Two kinds of separated flows can be recognized, that is fully separated flow and annular flow: while the former consists of two single phase streams (and occurs at low velocity flow of gas and liquid), in an annular flow the droplets are an important feature and, therefore, it can be regarded as only partially separated.

The derivation of the equations for multi-phase flows is considerably more complicated than for single-phase flows. This can be primarily ascribable to the presence of multiple, deformable and moving interfaces, across which the fluid properties can vary significantly.

The solution of a multi-phase flow field can be performed by following two different approaches, that is the two-fluid model and the mixture model. For the *two-fluid model*, the single-phase fluid flow governing equations are solved for both phases and are then coupled by setting appropriate kinematic and dynamic conditions at the interface. In the *mixture model*, the different phases are treated as a single fluid with variable properties and the conservation equations are solved for the mixture.

In theory, a two-phase flow problem can be formulated in terms of the local instant variables. However, there are considerable mathematical difficulties in following this approach, since a multiboundary problem would results, for which the positions of the interface is unknown due to the coupling of the fields and the boundary conditions. Concisely, the great difficulties for employing the local instant formulation come from the existence of the multiple deformable and moving interfaces, the fluctuations of variables due to turbulence and to the motions of the interfaces, and the significant discontinuities of properties at interface. Therefore, it is a common practice to apply some sort of averaging thus to effectively eliminate the local instant fluctuations and obtain the mean values of fluid motions and properties.

For the modeling of a discrete phase (small bubbles, solid particles or drops) co-flowing with a background fluid, two kinds of models are prevalent, that is the trajectory model and the two-fluid model. In *trajectory models*, also known as *Lagrangian* approaches, the motion of the disperse phase is determined by following the motion of each particle (or the motion of larger, representative particles) through a reference frame which moves with the particles themselves.

In *two-fluid models*, also known as *Eulerian* approaches, the discrete nature of the disperse phase is neglected and its effects on the carrier medium are approximated like another fluid acting on the continuous phase. In this case, the reference frame is stationary and the particles pass through fixed differential control volumes.

2   Characterization of multi-phase flows

In fluid mechanics, a multi-phase flow can be defined as a flow system in which two or more distinct phases flow simultaneously, having some level of phase separation at a scale well above the molecular level.

It is worth pointing out the distinction between multiphase flows and multicomponent flows: while the latter consist of a mixture of chemical species, mixed at the molecular level, the fluids in a multiphase flow are assumed to be mixed at macroscopic length scales, much larger than the molecular one. The fluids may interact with each other by means of interfacial forces and heat and mass transfer across the phase interfaces.

As suggested in [5], two-phase flows are fundamentally multi-scale in nature. At least four different scales can be recognized: the system scale, the macroscopic scale (required for continuum assumption), the mesoscale (related to local structures) and the microscale scale (related to fine structures and molecular transport).

The immiscibility of two fluids results from the strong cohesion forces existing between their molecules, and depends on the nature of the fluids. The easiness of mixing is generally expressed through the surface tension: the larger the value of this coefficient, the stronger the resistance to the mixing.

Multi-phase flows can, in general, exist in many different forms. For instance, two-phase flows can be classified according to the state of the phases as *gas-solid* flows, *liquid-solid* flows or *gas-liquid* flows. Moreover, a further group can be identified, that is *immiscible-liquid* mixture: even though it is not a real two-phase flow, for all practical purposes it can be treated as if it were a two-phase mixture.

Gas-solid flows regard with the motion of suspended solids or droplets in the gas phase. Gas-particle flows can be referred to as dispersed flows in which the solid particles constitute the dispersed phase, while the gas forms the continuous phase. The behaviour of the system depends on the particle number density, and three different regimes can be detected. In *dilute gas-particle flows* the influence of the gas flow is the dominant effect and the motion of the particles is governed by the surface and body forces acting on them. On the contrary, when the particle number density is sufficiently large, the motion of the particles is mainly influenced by particle-particle interactions. This kind of flow is referred as *dense gas-particle flows*. A special case of the dilute regime is offered by the *very dilute gas-particle flows*, for which the solid particles act as tracers and do not affect the gas flow. Examples of gas-solid flows are smoke and flow in pneumatic conveyers.

Liquid-solid flows deal with the transport of solid particles in a liquid phase and can also be categorized as dispersed flows, for which the liquid represents the continuous phase. In comparison to gas-particle flows, the liquid and solid phases are mainly driven by the pressure gradients, since the density ratio between phases is normally low while there is a significant inter-phase drag. Examples of liquid-solid flows are provided by the sediment transport of sand in rivers and the flows in wastewater treatment plants.

The gas-liquid flow is regarded as the most complex type which can be encountered in nature and industrial processes, since it combines the characteristics of a deformable interface and the

compressibility of the gas phase (bubbles and droplets are free to deform and, therefore, can assume different geometrical shapes, e.g., spherical, elliptical, cap and so on).

A special case of immiscible-liquid flows is provided by *free surface flows*, for which a further complication comes from the presence of well defined interfaces. Free surface flows are usually treated with both phases considered as continuous.

The singular characteristic of two-phase or immiscible flows is the presence of one or several interfaces separating each phase or components. Hence, besides the classification based on the combinations of the phases, two-phase flows can be classified according to the geometry of the interfaces into three main classes, namely, dispersed flows, separated flows and transitional or mixed flows, as illustrated in Fig. 1. Since the change of interfacial structures occurs gradually, transitional flows are characterized by the presence of both separated and dispersed flows. The transition happens frequently for liquid-vapor mixtures, as a consequence of the phase change along a channel. As Fig. 1 suggests, for each group several sub-classes can be identified. In the
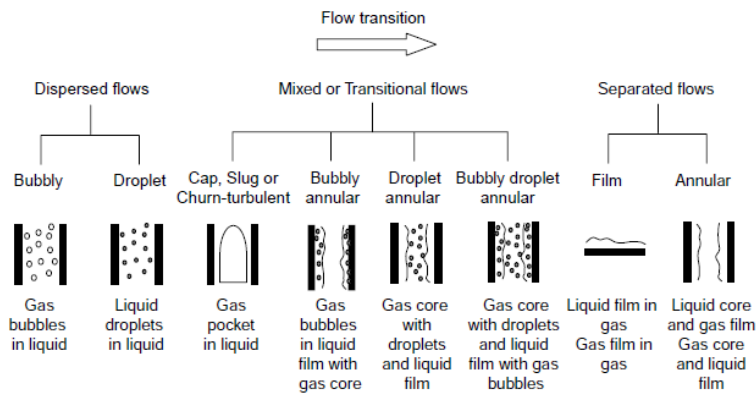
Figure 1: Classification of two-phase flows. From [10].
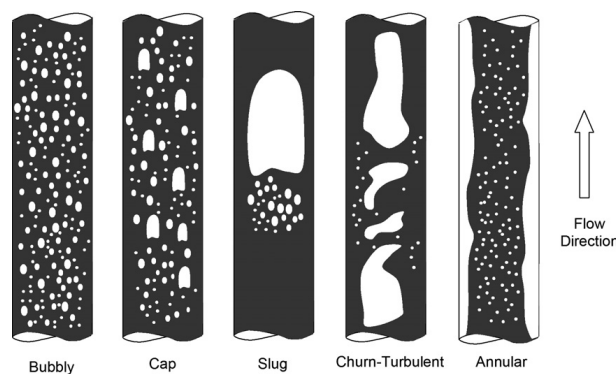
Figure 2: Classification of gas-liquid flows. From [9].

following part of this Section, the most common flow regimes for vertical and horizontal pipes will be illustrated.

With reference to Fig. 2, the different kinds of interfacial distributions in a vertical pipe can be categorized into five types, that is bubbly flow, cap flow, slug flow, churn-turbulent flow and annular flow.

In a *bubbly flow*, the gas phase is distributed in the continuous liquid phase as discrete bub-

bles, smaller than the tube diameter. When the superficial velocity[1] of the gas phase increases, deformed or elongated bubbles become more prevalent and cap bubbles are formed (*cap flow* regime), which are precursors to the formation of slug units in the slug flow regime.

The *slug flow* regime is characterized by the presence of bullet shaped gas bubbles, the so called *Taylor bubbles*, elongated in the direction of the channel axis. These bubbles present a characteristic hemispherical cap and abruptly terminate at the bottom edge. Their length can vary from one diameter up to several channel diameters. Between the channel wall and gas bubble a thin liquid film is present, which flows in the opposite direction of the plug motion. The Taylor bubbles are separated by liquid slugs, which can contain, occasionally, some small bubbles [1]. This slug pattern is often avoided in the design since it causes undesirable flow instability [10]. The drag for the bubbles in the slug flow regime differs substantially from that in the bubbly flow regime, due to the different size and shape of the bubbles.

At even higher gas velocities, large unsteady gas volumes tend to accumulate and produce the *churn-turbulent flow* regime. The Churn flow can defined as a slug flow characterized by high level of disorder: the bubbles are, in fact, narrower and distorted, their diameter is smaller than the channel's diameter and the liquid-gas interface is more irregular. The liquid slugs between two consecutive elongated bubbles are characterized by a high concentration of gas. In this regime, the liquid phase can flow up and down in an oscillatory manner.

In the *annular flow*, the gas phase flows along the channel axis, while the liquid flows in the same direction as a liquid film attached to the channel walls. In the gas core, some liquid droplets can be detected, which are originated from the rupture of the wavy gas-liquid interface. At even higher gas velocities, a *disperse* pattern can be identified, in which a considerable amount of liquid bubbles flow in the gas core.
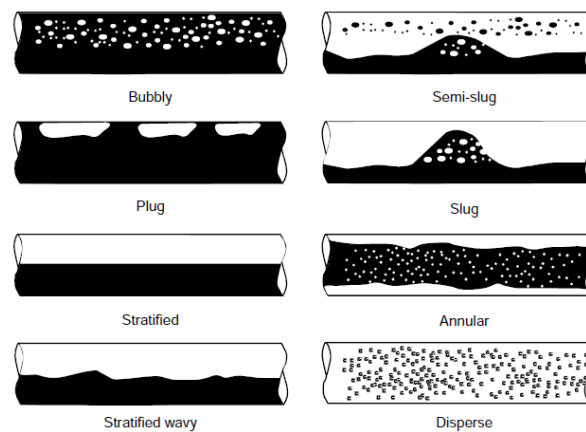
Figure 3: Classification of gas-liquid flows. From [10].

In horizontal ducts, the phases tend to separate due to differences in density: therefore, stratified flows are very often encountered. In Fig. 3, the flow regimes for a gas-liquid flow in a horizontal duct are illustrated. In the *bubbly flow* regime, the dispersed gas bubbles tent to migrate towards the top of the pipe; when the fluid velocity is risen, the turbulence level increases and causes bubbles to be more uniformly distributed across the tube. Such behaviour is also observed for the *plug flow* regime at low gas flow rates. The plug flow is an intermittent regime, since liquid plugs, free of entrained gas, are separated by zones of elongated gas bubbles. In the *stratified*

---

[1]In a multi-phase flow, the superficial velocity corresponds to the velocity that the fluid would have if it were the only one flowing in a given cross sectional area.

flow regime, a clear separation of the two phases can be observed, with the liquid flowing along the lower surface. This flow regime occurs at low liquid and gas velocities. When the gas velocity is increased, the smooth interface between the two phases becomes wrinkled and, therefore, the stratified wavy sub-regime can be identified. The amplitude of the waves depends on the relative velocity between the phases and the properties of the fluid such as density and surface tension [10]. When the gas velocity is further risen, the wave amplitude increases and waves can touch the top of the tube: when this occurs, the *slug flow* regime is established. The liquid slugs between the air bubbles can contain small bubbles. With respect to the plug flow, this regime is more chaotic and the interface between the liquid slugs and the gas bubbles is not so sharp. Also the slug flow can be referred as an intermittent flow.

At higher gas flow rates, a transition to the *annular flow* regime takes place. In this case, a liquid film is formed on the pipe wall, somewhat similar to that observed in vertical co-current flow, with the exception that the film at the bottom may be much thicker than that at the top. In analogy to the vertical pipe, the interface may be wavy and dispersed liquid droplets can be detected in the gas core. At even higher gas flow rates, a *disperse flow* regime is subsequently formed.

(a)   (b)
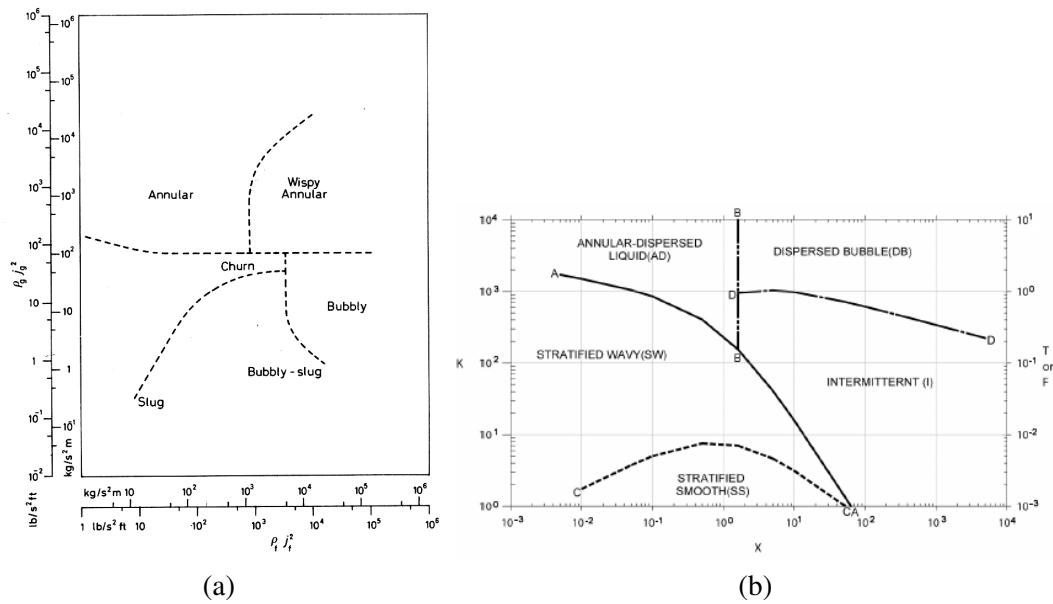
Figure 4: (a) Flow pattern map obtained by Hewitt and Roberts for two-phase co-current upwards flow in a vertical tube. (b) Flow pattern map obtained by Taitel and Dukler for horizontal co-current flows.

The common practice in representing flow-pattern data is to plot the data as a two-dimensional flow-pattern map[2]. Many flow pattern maps have been developed for gas-liquid flow in horizontal and vertical tubes. For vertical tubes with upward flow, the most-used flow pattern map is that of Hewitt and Roberts[3], illustrated in Fig. 4(a), and developed for air-water flows. For hori-

---

[2]For further information, please refer to [3]

[3]In Fig. 4(a), j_i represents the volumetric flux for the i-th phase, defined as:

$$j_i = \frac{G_i}{\rho_i} = \frac{\dot{m}_i}{A\rho_i} \quad \left[\frac{\text{m}^3}{\text{m}^2 \cdot \text{s}}\right] \tag{1}$$

zontal and near horizontal tubes, a well known flow map is that proposed by Taitel and Dukler[4], as illustrated in Fig. 4(b).

Figure 5: Effect of an increased air input fraction on a three-phase flow, $J_o = 0.46$m/s and $J_w = 0.32$m/s. Photographies taken by the research team of Prof. Sotgia (Politecnico di Milano).
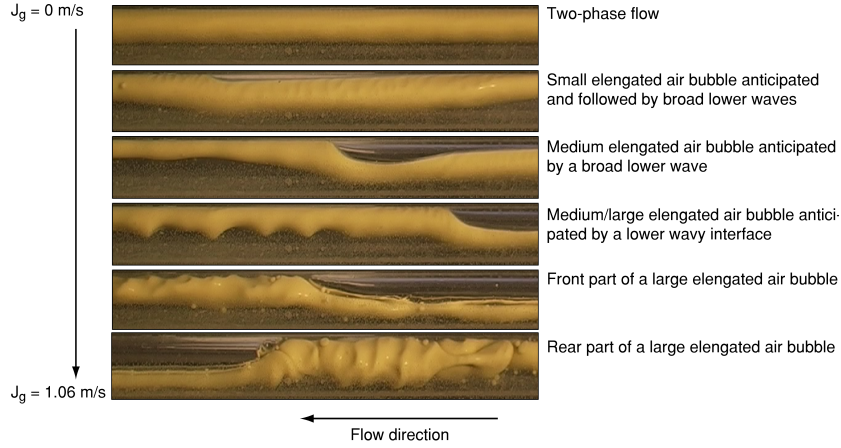
In many engineering applications, three-phases flows are also encountered. As an example, we can mention the oil transportation in pipelines: in these cases, besides the common practice of adding some water in order to reduce the pressure drop, an unwanted evaporation of the lighter hydrocarbons can occur, thus producing a gaseous phase in the pipeline. It is obvious that the presence of the third phase increases the complexity of the flow pattern. As quoted in [7], a possible way to study this kind of multi-phase flow is to investigate the influence of a third phase (air) on liquid-liquid two phase flow. In some cases the three-phase flow can be described as a liquid-liquid core annular or liquid-liquid stratified flow on which elongated droplets are present. In other conditions the three-phase flow patterns differs completely from the liquid-liquid one.

Figure 5 shows the experimental visualizations of a three-phases oil-water-gas flow with the increase of the gas superficial velocity[5]. It can be seen that, at low gas input fraction, the three-phase flow appears as a modification of the reference two-phase one. By increasing the gas flux, some elongated gas bubbles appear in the upper part of the tube, which gradually increase in size. At the same time, the interface between oil and water starts to wrinkle. In the limiting

---

being G_i is the mass flux for the i-th phase $\left[\mathrm{kg}/(\mathrm{m}^2 \cdot \mathrm{s}) \right]$.

   [4]Without going into details, the dimensionless parameters employed in the Teitel-Dukler map are the following:

$$X^2 = \frac{(dp/dz)_{SL}}{(dp/dz)_{SG}} \quad \text{Martinelli parameter}$$

$$T = \sqrt{\frac{|(dp/dz)_{SL}|}{(\rho_L - \rho_G)g\cos\theta}} \quad \text{dispersed bubble flow parameter}$$

$$F = \sqrt{\frac{\rho_G}{\rho_L - \rho_G}} \frac{u_{SG}}{\sqrt{Dg\cos\theta}} \quad \text{modified Froude number}$$

$$K = F\sqrt{\frac{Du_{SL}}{\nu_L}} \quad \text{wavy flow parameter}$$

with: SL superficial liquid, SG superficial gas, D inner diameter of the tube, θ inclination angle of the pipe.

   [5]J_o: superficial velocity of the oil phase, J_w superficial velocity of the water phase, J_g superficial velocity of the gas phase.

case, if the gas superficial velocity were further increased, then the oil core would break into a kind of core of dispersed drops.

The complexity of the motion of a dispersed system is connected to several phenomena which can occur, as the the change in shape or diameter of the bubbles, coalescence, dispersion and breakup, collisions between particles and collisions of the particle with the wall. Moreover, heat and mass transfers across the phases can take place, just like the establishment of turbulent phenomena.

3   Numerical modeling of multi-phase flows

In multi-phase flows, the presence of interfacial surfaces introduces great difficulties in formulating the problem. From a mathematical point of view, a multiphase flow can be regarded as a field subdivided into single-phase regions with moving boundaries separating the constituent phases. The differential balances are valid for each sub-region. From the point of view of physics, the difficulties encountered in deriving the constitutive equations arise from the presence of the interfaces, and can be basically ascribable to three aspects. The interfaces are, in fact, deformable and their motions are unknown: this fact causes complicated coupling between the field equations of each phase and the interfacial conditions. Moreover, significant discontinuities of properties at interface may occur, which introduce huge local jumps in various variables in space and time. In addition, fluctuations of the field variables may exist, due to turbulence and to the motions of the interfaces[6].

In theory, it is possible to formulate a two-phase flow problem in terms of the local instant variables (the so called *local instant formulation*)[7], which is equivalent to a Direct Numerical Simulation (DNS). However, the microscopic motions and thermal characteristics of the individual constituents are, in general, complex and difficult to recover (there is an uncertainty in finding the exact locations of the constituents at a specific time). Furthermore, for most practical purposes, the exact prediction of the evolutionary behaviour of a system is not necessary. Therefore, in the derivation of the effective conservation equations, it is customary to apply some sort of averaging process[8]. By proper averaging, the mean values of fluid motions and properties can be obtained, which effectively eliminate the local instant fluctuations: in this way, the predictions are restricted to macroscopic phenomena. The averaging procedure can be considered as low-pass filtering, excluding unwanted high frequency signals from local instant fluctuations [5].

Generally, averaging may be performed in time, space, over an ensemble or in some combination of these. With reference to an instantaneous field $\phi(x, y, z, t)$, the aforementioned averaging approaches can be defined as:

- Time average

$$\bar{\phi} = \lim_{T \to \infty} \frac{1}{T} \int \phi(x, y, z, t) dt \quad \bar{\phi} = \bar{\phi}(x, y, z) \tag{2}$$

---

[6]It is worth noting that, even multiphase flows that are not turbulent in the strictest sense will exhibit variations in the velocities due the flows around particles. When multi-phase flows become turbulent, they will also exhibit conventional Reynolds stresses.

[7]The local instant formulation is important for several problems, i.e., bubble's dynamics, growth or collapse of a single bubble or a droplet, and ice formation and melting.

[8]It is worth noting that even in single-phase turbulent flow without moving interfaces it is not possible to obtain exact solutions expressing local instant fluctuations.

- Space average

$$\langle\phi\rangle_V = \lim_{V\to\infty} \frac{1}{V} \int \phi(x,y,z,t)dt \quad \langle\phi\rangle_V = \langle\phi\rangle\,(t) \tag{3}$$

- Ensemble average

$$\langle\phi\rangle_E = \lim_{N\to\infty} \frac{1}{N} \sum_{n=1}^{N} \phi_n(x,y,z,t)dt \quad \langle\phi\rangle_E = \langle\phi\rangle\,(x,y,z,t) \tag{4}$$

The time averaging is particularly useful for a turbulent two-phase flow or for a dispersed two-phase flow, since the transport processes are highly dependent on the local fluctuations of variables about the mean.

As it can be appreciated from Eq.(4), the ensemble averaging is is defined by an arithmetic mean among a set of N similar samples or systems.

The solution of a multi-phase flow field can be performed by following two different approaches, that is the two-fluid model and the mixture model. The *two-fluid model* is formulated by considering each phase separately: two sets of conservation equations are solved and then coupled through appropriate conditions at the interface. Two-fluid modeling proceeds by averaging the local instantaneous conservation equations for mass, momentum and energy over each phase.

On the other hand, the *mixture model* considers the mixture as a single fluid with variable properties. The model is expressed in terms of three-mixture conservation equations with one additional diffusion (continuity) equation, which takes account of the concentration changes[9].

Liquid-particle flows can generally be viewed as a "mixed flow" since the densities between the liquid and solid particles are not rather dissimilar: in this way, the multi-phase problem can be treated as a single-fluid formulation (mixture model).

On the contrary, in many multi-phase problems associated with gas-particle flows, the two-fluid formulation is adopted: the disperse phase can be handled by applying either the Eulerian or Lagrangian strategy, while the continuous phase is solved via the Eulerian approach. For bubbly flows, the two-fluid is invariably employed due to the complex mechanistic behaviours (collision and merging of adjacent bubbles, shearing of the bubbles by the turbulent eddies, and evaporation/condensation phenomena).

As pointed out in [10], the ability of a two-fluid model to predict a multiphase flow depends on the goodness of the closure relationships formulated for the various inter-phase interaction properties, such as the interfacial mass, momentum and energy exchanges. In fact, at the interface, a particular form of the balance equation should be used, in order to account for the the sharp changes (or discontinuities) in various variables. For this purpose, the so-called jump conditions have been developed[10], which specify the exchanges of mass, momentum, and energy through the interface.

In Section 4, the constitutive equations for the two-fluid model are introduced, while the mixture model is described in Section 5.

---

[9]As it will be seen, the further equation is formulated for the volume-average phase indicator function.

[10]The derivation of the jump conditions is omitted in these notes.

4   Two-fluid model

The two-fluid model allows, for each point in the space, the coexistence of both phases through two separate velocity fields and a scalar variable, accounting for the volume fraction occupied by the reference phase. As already explained, in view of the difficulty in handling the instantaneous local values of flow variables, an averaging process is applied to the local instantaneous conservation equations for mass, momentum and energy over each phase, in order to trace the macroscopic phenomena of the fluid field.

In this way, a representative element of volume dV is chosen, which is composed by a mixture of phases: the sub-volume occupied by the k-phase can be indicated as dV^k. Afterwards, the microscopic quantities are first averaged on the representative volume dV, and then time averaged.

4.1   Conservation of Mass

In a multi-phase flow, the local instantaneous equation for the conservation of mass of the k-th phase can be formulated by taking into account the corresponding equation for a single-phase flow:

$$\frac{\partial \rho^k}{\partial t} + \nabla \cdot (\rho^k \mathbf{U}^k) = 0 \tag{5}$$

Moreover, to distinguish the different phases that are present within the fluid flow, a *phase indicator function* $\chi^k(x, y, z, t)$ can be introduced, defined as:

$$\chi^k(x, y, z, t) = \begin{cases} 1, & \text{if } (x, y, z) \text{ is in } k\text{-th phase at time } t, \\ 0, & \text{otherwise} \end{cases} \tag{6}$$

and

$$\nabla \chi^k = \mathbf{n}^k \delta(\mathbf{x} - \mathbf{x}^{int}, t) \tag{7}$$

As it can be seen, $\nabla \chi^k$ is a *generalized function* which behaves like a Dirac δ function. A generalized function allows to express in a mathematically-corrected form some idealized concepts, as the density of a point or the intensity of an instantaneous source. This reflects the fact that, in reality, a physical quantity cannot be measured at a point but only its mean values can be measured, over sufficiently small neighbourhoods of the given point.

From Eq.(7) it follows that both the partial derivatives of the phase indicator function vanish away from the interface (i.e., $\nabla \chi^k \neq 0$ only at the interface).

The phase indicator function owns the following properties:

$$\sum_{k=1}^{M} \chi^k = 1 \tag{8}$$

being M the number of phases of the flow, and:

$$\frac{D\chi^k}{Dt} = \frac{\partial \chi^k}{\partial t} + \mathbf{U}^{int} \cdot \nabla \chi^k = 0 \tag{9}$$

where $\mathbf{U}^{int}$ is the velocity of the interface. If a inter-phase mass transfer occurs across the interface, the motion of the interface is provided not only by convection but also by the amount

of mass being transferred between the fields.

The phase indicator function is also useful for defining the volume dV^k of the representative element of volume occupied by the k-phase:

$$dV^k = \int_{dV} \chi^k dV \tag{10}$$

and, then, the integral of a function f over dV^k:

$$\int_{dV^k} f dV^k = \int_{dV} f\chi^k dV \tag{11}$$

As it will be seen later, the above properties are useful for defining two average operator, a volume average operator:

$$\langle f \rangle = \frac{1}{dV} \int_{dV} f\chi^k dV \tag{12}$$

and a mass average operator:

$$\overline{f} = \frac{\int_{dV} \rho f \chi^k dV}{\int_{dV} \rho \chi^k dV} = \frac{1}{\langle\rho\rangle \, dV} \int_{dV} \rho f \chi^k dV \tag{13}$$

By multiplying Eq.(5) by χ^k it results:

$$\chi^k \frac{\partial \rho^k}{\partial t} + \chi^k \nabla \cdot (\rho^k \mathbf{U}^k) = 0 \tag{14}$$

and then, by considering Eq.(9)[11]:

$$\frac{\partial(\chi^k \rho^k)}{\partial t} + \nabla \cdot (\chi^k \rho^k \mathbf{U}^k) = \rho^k \left(\mathbf{U}^k - \mathbf{U}^{int} \right) \cdot \nabla \chi^k \tag{15}$$

The averaged form of the conservation of mass can be obtained by applying an averaging process[12] to Eq.(15):

$$\left\langle \frac{\partial(\chi^k \rho^k)}{\partial t} \right\rangle + \left\langle \nabla \cdot (\chi^k \rho^k \mathbf{U}^k) \right\rangle = \left\langle \rho^k \left(\mathbf{U}^k - \mathbf{U}^{int} \right) \cdot \nabla \chi^k \right\rangle$$

$$\Rightarrow \frac{\partial \left\langle \chi^k \rho^k \right\rangle}{\partial t} + \nabla \cdot \left\langle \chi^k \rho^k \mathbf{U}^k \right\rangle = \underbrace{\left\langle \rho^k \left(\mathbf{U}^k - \mathbf{U}^{int} \right) \cdot \nabla \chi^k \right\rangle}_{\Gamma^k} \tag{16}$$

The term on the right-hand side of Eq.(16), Γ^k, represents the interfacial mass source, corresponding to the mass transfer toward the k phase at the interface. It is outstanding that this term must be considered only in the event of mass transfer between the phases.

Since no storage or accumulation is realized at the interface, it must result:

$$\sum_{k=1}^{M} \Gamma^k = 0 \tag{17}$$

---

[11]Some simple mathematical steps are omitted.

[12]Either the volume averaging or ensemble averaging could be employed to formulate the averaged conservation equations, since both of them result essentially in the same form of equations. Therefore, the generic averaging process will be denoted as $\langle \cdot \rangle$.

Equation (17) expresses the conservation of mass at the interfaces.

Equation 16 was obtained by assuming the averaging process satisfies the following rules:

$$
\begin{aligned}
\langle\langle a\rangle\rangle &= \langle a\rangle \\
\langle a + b\rangle &= \langle a\rangle + \langle b\rangle \\
\langle\langle a\rangle\, b\rangle &= \langle a\rangle\,\langle b\rangle \\
\left\langle\frac{\partial a}{\partial t}\right\rangle &= \frac{\partial\langle a\rangle}{\partial t} \\
\left\langle\frac{\partial a}{\partial x_j}\right\rangle &= \frac{\partial\langle a\rangle}{\partial x_j} = \nabla\langle a\rangle
\end{aligned}
\tag{18}
$$

4.2   Conservation of Momentum

Also the local instantaneous equation for the conservation of momentum of the k-th phase can be formulated by taking into account the corresponding equation for a single-phase flow:

$$
\rho^k\frac{\partial\mathbf{U}^k}{\partial t} + \rho^k\mathbf{U}^k\cdot\nabla\mathbf{U}^k = -\nabla p^k + \nabla\cdot\tau^k + \sum\mathbf{F}^{k,\ body\ forces}
\tag{19}
$$

where τ^k denotes the extra stresses tensor. Examples of body forces are provided by gravity and electromagnetical forces. The body force due to gravity is the most common one and, therefore, the last term of Eq.(19) can be formulated as:

$$
\mathbf{F}^{k,\ body\ forces} = \rho^k\mathbf{g}
\tag{20}
$$

In a way analogous to the derivation of the averaged equation for the conservation of mass, the averaged equation governing the conservation of momentum can be obtained:

$$
\frac{\partial\left\langle\chi^k\rho^k\mathbf{U}^k\right\rangle}{\partial t} + \nabla\cdot\left\langle\chi^k\rho^k\mathbf{U}^k\otimes\mathbf{U}^k\right\rangle = -\nabla\left\langle\chi^k p^k\right\rangle + \nabla\cdot\left\langle\chi^k\tau^k\right\rangle + \left\langle\chi^k\right\rangle\left\langle\sum\mathbf{F}^{k,\ body\ forces}\right\rangle
$$
$$
+ \underbrace{\left\langle\rho^k\mathbf{U}^k\left(\mathbf{U}^k - \mathbf{U}^{int}\right)\cdot\nabla\chi^k\right\rangle}_{\Gamma^k} + \left\langle p^k\right\rangle\left\langle\nabla\chi^k\right\rangle - \left\langle\tau^{\mathbf{k}}\cdot\nabla\chi^k\right\rangle
$$
$$
\underbrace{\hspace{10cm}}_{\Omega^k}
\tag{21}
$$

The term $\nabla\cdot\left\langle\chi^k\tau^k\right\rangle$ comprises the stress tensor[13], while Ω^k accounts for the interfacial momentum source. In particular, $\Gamma^k = \left\langle\rho^k\mathbf{U}^k\left(\mathbf{U}^k - \mathbf{U}^{int}\right)\cdot\nabla\chi^k\right\rangle$ represents the interfacial momentum due to mass exchange across interface, while the quantity $\left\langle\rho^k\right\rangle\left\langle\nabla\chi^k\right\rangle - \left\langle\tau^{\mathbf{k}}\cdot\nabla\chi^k\right\rangle$ stands for the interfacial force density. From a physical consideration, the interfacial force density contains forces acting on the dispersed phase due to viscous drag, wake and boundary-layer formations, and the unbalanced pressure distributions leading to the well-known effects of added or virtual mass, lift and Bassett history contribution[14].

The average interfacial momentum balance constraint gives:

$$
\sum_{k=1}^{M}\Omega^k \equiv F_\sigma
\tag{22}
$$

---

[13]In the event of a turbulent flow, the turbulent component of the stresses is included in τ^k.

[14]All these forces will be described later.

where F_σ is the interfacial momentum source, which is the contribution to the total force on the mixture given by the surface tension at the interface.

4.3 Conservation of Energy

Among the many different forms governing the conservation of energy, the total enthalpy equation represents a convenient form that is most frequently employed in multi-phase flow investigations. The local instantaneous equation for the k-th phase can be formulated as:

$$\rho^k \frac{\partial H^k}{\partial t} + \rho^k \mathbf{U}^k \cdot \nabla H^k = -\frac{\partial p^k}{\partial t} - \nabla \cdot \mathbf{q}^k + \sum \mathbf{F}^{k,\, body\, forces} \cdot \mathbf{U}^k + \Phi_H^k \tag{23}$$

where $\Phi_H^k = \nabla \cdot (\mathbf{U}^k \cdot \tau^k)$.
The average form of the energy equation is the following:

$$\begin{aligned}
\frac{\partial \left\langle \chi^k \rho^k H^k \right\rangle}{\partial t} + \nabla \cdot \left\langle \chi^k \rho^k \mathbf{U}^k H^k \right\rangle = &-\frac{\partial \left\langle \chi^k p^k \right\rangle}{\partial t} - \nabla \cdot \left\langle \chi^k \mathbf{q}^k \right\rangle \\
&+ \left\langle \chi^k \right\rangle \left\langle \sum \mathbf{F}^{k,\, body\, forces} \cdot \mathbf{U}^k \right\rangle + \left\langle \Phi_H^{\prime k} \right\rangle \\
&+ \underbrace{\left\langle \rho^k H^k \left(\mathbf{U}^k - \mathbf{U}^{int} \right) \cdot \nabla \chi^k \right\rangle + \left\langle \mathbf{q}^k \nabla \chi^k \right\rangle + \left\langle p^k \right\rangle \left\langle \frac{\partial \chi^k}{\partial t} \right\rangle + \left\langle \Phi^{extra} \right\rangle}_{\Pi_H^k}
\end{aligned}$$

$$\tag{24}$$

The terms $\left\langle \Phi_H^{\prime k} \right\rangle$ and $\left\langle \Phi^{extra} \right\rangle$ are the viscous contributions, defined as:

$$\left\langle \Phi_H^{\prime k} \right\rangle = \nabla \cdot \left\langle \chi^k \mathbf{U}^k \cdot \tau^k \right\rangle \tag{25}$$

$$\left\langle \Phi^{extra} \right\rangle = - \left\langle \mathbf{U}^k \cdot \tau^k \cdot \nabla \chi^k \right\rangle \tag{26}$$

The term Π_H^k corresponds to the interfacial energy transfer. The quantity $\left\langle \rho^k H^k \left(\mathbf{U}^k - \mathbf{U}^{int} \right) \cdot \nabla \chi^k \right\rangle$ represents the interfacial energy due to mass exchange across the interface, $\left\langle \mathbf{q}^k \nabla \chi^k \right\rangle$ characterizes the flux of heat being transferred into the k-th phase from the other phases normal to the interface, $\left\langle \rho^k \right\rangle \left\langle \frac{\partial \chi^k}{\partial t} \right\rangle$ depicts the interfacial work due to the pressure, while $\left\langle \Phi^{extra} \right\rangle$ the extra stresses acting on the interface.
The interfacial energy balance constraint for the total enthalpy gives:

$$\sum_{k=1}^{M} \Pi_H^k \equiv \varsigma \tag{27}$$

where ς is the interfacial energy source, produced by the work done by the surface tension at the interface:

$$\varsigma = F_\sigma \cdot U^{int} \tag{28}$$

being U^{int} the interfacial velocity.

4.4   Effective Conservation Equations

The specific forms of the averaged conservation equations illustrated so far involve averages of products of local instantaneous dependent variables (i.e., $\langle \chi^k \rho^k \rangle$) and, therefore, can not be solved directly. One possible approach to reduce the *averages of products* to *products of averages* is to consider the separation of the mean flow from the fluctuating quantities. This is analogous to further averaging the governing equations in time in order to suppress the fluctuating fields[15].

In a multi-phase flow analysis, the *Favre-averaging approach* is usually employed, and two types of averaged variables can be used. The *phase-weighted average* for the variable ϕ can be defined by:

$$\overline{\langle \phi \rangle} = \frac{\overline{\langle \chi^k \phi \rangle}}{\overline{\langle \chi^k \rangle}} \tag{29}$$

while the *mass-weighted average* of the variable ψ is the following:

$$\overline{\langle \psi \rangle} = \frac{\overline{\langle \rho^k \phi \rangle}}{\overline{\langle \rho^k \rangle}} \tag{30}$$

The instantaneous volume-averaged or ensemble-averaged variables of ϕ and ψ can be written as:

$$\langle \phi \rangle = \overline{\langle \phi \rangle} + \phi'' \tag{31a}$$

$$\langle \psi \rangle = \overline{\langle \psi \rangle} + \psi'' \tag{31b}$$

where ϕ'' and ψ'' are the superimposed fluctuations. By multiplying Eq.(31a) and (31b) by $\langle \chi^k \rangle$ and $\langle \rho^k \rangle$, respectively, it is fair to write:

$$\left\langle \chi^k \phi \right\rangle = \left\langle \chi^k \right\rangle \overline{\langle \phi \rangle} + \left\langle \chi^k \right\rangle \phi'' \tag{32a}$$

$$\left\langle \rho^k \psi \right\rangle = \left\langle \rho^k \right\rangle \overline{\langle \psi \rangle} + \left\langle \rho^k \right\rangle \psi'' \tag{32b}$$

In this way, the average of the product of instantaneous local quantities, $\langle \chi^k \phi \rangle$, has been transformed into the sum of a product of two average quantities, $\langle \chi^k \rangle \overline{\langle \phi \rangle}$, and a product of an average and a fluctuating quantity $\langle \chi^k \rangle \phi''$. In analogy with what was seen for single-phase turbulent flows, in order to free from the fluctuating quantity, a time average[16] can be performed and, therefore, the above equations can be reduced to:

$$\overline{\langle \chi^k \phi \rangle} = \overline{\langle \chi^k \rangle} \, \overline{\langle \phi \rangle} + \overline{\langle \chi^k \rangle \phi''} \tag{33a}$$

$$\overline{\langle \rho^k \psi \rangle} = \overline{\langle \rho^k \rangle} \, \overline{\langle \psi \rangle} + \overline{\langle \rho^k \rangle \psi''} \tag{33b}$$

Now, on the basis of the definitions of the phase-weighted and mass-weighted averages, it follows that:

$$\overline{\langle \chi^k \rangle \phi''} = 0 \tag{34a}$$

$$\overline{\langle \rho^k \rangle \psi''} = 0 \tag{34b}$$

---

[15]The necessity of time-averaging the averaged conservation equations is similar to that for turbulent single-phase flows.

[16]It is well known that the time-average of the fluctuating components, $\overline{\psi''}$, is zero.

and hence:

$$\overline{\langle \chi^k \rangle \phi} = \overline{\langle \chi^k \rangle} \, \overline{\langle \phi \rangle} \tag{35a}$$

$$\overline{\langle \rho^k \rangle \phi} = \overline{\langle \rho^k \rangle} \, \overline{\langle \phi \rangle} \tag{35b}$$

Equation (35) provides the relations for transforming an average of products into a product of averages.

In the event where the governing equations are first volume-averaged and then time-averaged, suitable forms of conservation equations via the phase-weighted and mass-weighted averages can be formulated. In this case, a new useful quantity can be introduced, that is the *local volume fraction* (or *local concentration*):

$$\alpha^k = \frac{V_k}{V} \tag{36}$$

α^k can be regarded as the ratio of the fractional volume V^k of the k-th phase in an arbitrary small region over the total volume V of the region in question within the two-phase flows. It also corresponds to the volume-averaged of the phase indicator function, that is, $\alpha^k = \langle \chi^k \rangle$.

In this way, dropping the bars and parentheses which by default denote the Favre-averaging and volume-averaging processes, the effective conservation equations written in terms of the local volume fraction and products of averages are the following:

Conservation of Mass:

$$\frac{\partial (\alpha^k \rho^k)}{\partial t} + \nabla \cdot (\alpha^k \rho^k \mathbf{U}^k) = \Gamma'^k \tag{37}$$

Conservation of Momentum[17]:

$$\frac{\partial (\alpha^k \rho^k \mathbf{U}^k)}{\partial t} + \nabla \cdot (\alpha^k \rho^k \mathbf{U}^k \otimes \mathbf{U}^k) = - \alpha^k \nabla p^k - p^k \nabla \alpha^k + \nabla \cdot (\alpha^k \tau^k) - \nabla \cdot (\alpha^k \tau^{k''})$$
$$+ \alpha^k \sum \mathbf{F}^{k, \, body \, forces} + \Omega'^k \tag{38}$$

Conservation of Energy:

$$\frac{\partial (\alpha^k \rho^k H^k)}{\partial t} + \nabla \cdot (\alpha^k \rho^k \mathbf{U}^k H^k) = p^k \frac{\partial \alpha^k}{\partial t} + \alpha^k \frac{\partial p^k}{\partial t} - \nabla \cdot (\alpha^k \mathbf{q}^k) - \nabla \cdot (\alpha^k \mathbf{q}_H^{k''})$$
$$+ \alpha^k \sum \mathbf{F}^{k, \, body \, forces} \cdot \mathbf{U}^k + \Phi_H^{``k} + \Pi_H'^k \tag{39}$$

where the mean total enthalpy is given by:

$$H^k = h^k + \frac{1}{2} \mathbf{U}^k \mathbf{U}^k + \frac{1}{2} \mathbf{U}^{``k} \mathbf{U}^{``k} \tag{40}$$

In the above equations, the term $\Phi_H^{``k}$ derives from the extra stresses, while Γ'^k, Ω'^k and $\Pi_H'^k$ are the interfacial terms generated by the Favre-averaging of the volume-average terms, Γ^k, Ω^k and Π_H^k. In CFD, the interfacial terms Γ'^k, Ω'^k and $\Pi_H'^k$ can be linearized for numerical treatment. It is worthwhile noting that, if ensemble averaging is performed on the governing equations, and fluctuating quantities are subsequently introduced into the equations, the final forms of the governing equations do not differ from those of the twice-averaged conservation equations [10].

---

[17] $\alpha^k \nabla p^k + p^k \nabla \alpha^k = \nabla (\alpha^k p^k)$

4.4.1   Comments on the governing equations

The key feature of the two-fluid model is that it can take into account the dynamic and non-equilibrium interactions between phases, since in its formulation two independent velocity fields as well as the two energy equations are allowed. However, in the case of strong coupling between the phases (e.g., the responses of phases are simultaneous such that they be considered close to mechanical and thermal equilibrium), the two-fluid model brings into the system unnecessary complications for practical applications.

The governing equations for multi-phase flows are "very much alike" to their single-phase counterparts, except for the local volume fraction and the additional source terms accounting for the inter-phase interactions.

The energy flux $\mathbf{q}^k$ resulting in the total enthalpy energy equation can normally be formulated by applying Fourier's law of heat conduction: $\mathbf{q}^k = -\lambda^k \nabla T^k$.

Two additional turbulent flux terms, the Reynolds stress $\alpha^k \tau^{k''}$ and the Reynolds flux $\mathbf{q}_H^{k''}$, results in Eq.38 and 39, which can be taken to be equivalent to the turbulent flux terms in single-phase turbulence problems. For closing the problem, a strategy similar to that already discussed for single-phase flows can be adopted.
Of course, in the absence of these terms, equations reduce to the description of a laminar fluid.

By examining the governing equations it is outstanding that, in the case of a two-phase flow, there are 16 unknowns, 8 for each phase (u^k, v^k, w^k, α^k, ρ^k, H^k, T^k and p^k). Under the hypotheses that the Reynolds stress and flux, as well as the interfacial exchange terms can be determined, Eq. 37, 38 and 39 provide a set of five equations for the computation of α^k, u^k, v^k, w^k and H^k, respectively. Moreover, for the evaluation of ρ^k the algebraic equation of state, $\rho^k = \rho^k(T^k, p^k)$, can be introduced, while the constitutive equation for the total enthalpy, $H^k = H^k(T^k, p^k)$, can be employed for computing T^k. A further condition is provided by the algebraic constraint for the local volume fraction, that is:

$$\sum_{k=1}^{M} \alpha^k = 1 \tag{41}$$

All the above cited equations form a set of 15 equations to close the two-fluid model. The remaining unknown, p^k, is usually computed by setting algebraic constraints on the pressure. As an example, if the difference between the velocities of the disperse and continuous phase (also referred to as the slip velocity) is small and no appreciable dispersed phase expansion/contraction occurs, one can assume that all phases share the same pressure field, that is $p^k = p$.

number	Equation	Solved variables
6	Momentum	$U^1, V^1, W^1, U^2, V^2, W^2$
2	Continuity	α^1, ρ^2
2	Energy	H^1, H^2
1	$\sum \alpha^k = 1$	α^2
2	Eq. of state	ρ^1, p^1
2	Constitutive Eq. for H	T^1, T^2
1	Constraint on p	p^2

Table 1: Equations employed for the computation of the unknowns for a two-phase flow.

A summary of the equations necessary for the computation of the unknowns for a two-phase

fluid is reported in Table 1.

As already mentioned, the success of a two-fluid model is strictly linked to the formulation of suitable constitutive equations for the interphase exchange terms, that is Γ'^{k}, Ω'^{k} and Π'^{k}_{H}, which is not a trivial task. In fact, it is impossible to find a set of equations universally valid for every flow pattern: therefore, some heuristic models will be employed for specific flow patterns.

5   Mixture model

As already explained, the *mixture model* is formulated by considering the mixture as a single fluid with variable properties. In other words, the mixture models englobes the conservation equations of the different phases into a single equation valid for the mixture. In this way, dynamic interaction of the phases does not occur since the interfacial exchange terms are omitted from the equations.

As pointed out in [5], the mixture model requires some drastic constitutive assumptions causing some of the important characteristics of two-phase flow to be lost. However, it is just its simplicity that makes it very useful in many engineering applications: in fact, information required is often the response of the total mixture and not of each constituent phase.

The mixture properties, e.g. density, viscosity and thermal conductivity, are evaluated from the corresponding properties of the two phases as:

$$\rho^{m} = \sum_{k=1}^{2} \alpha^{k} \rho^{k}, \quad \mu^{m} = \sum_{k=1}^{2} \alpha^{k} \mu^{k}, \quad \lambda^{m} = \sum_{k=1}^{2} \alpha^{k} \lambda^{k} \tag{42}$$

Moreover, the mixture velocity and enthalpy are treated as a combination of phase-weighted and mass-weighted variables:

$$\mathbf{U}^{m} = \frac{\displaystyle\sum_{k=1}^{2} \alpha^{k} \rho^{k} \mathbf{U}^{k}}{\displaystyle\sum_{k=1}^{2} \alpha^{k} \rho^{k}} = \frac{\displaystyle\sum_{k=1}^{2} \alpha^{k} \rho^{k} \mathbf{U}^{k}}{\rho^{m}}, \quad H^{m} = \frac{\displaystyle\sum_{k=1}^{2} \alpha^{k} \rho^{k} H^{k}}{\displaystyle\sum_{k=1}^{2} \alpha^{k} \rho^{k}} = \frac{\displaystyle\sum_{k=1}^{2} \alpha^{k} \rho^{k} H^{k}}{\rho^{m}}, \tag{43}$$

The conservation equations for the mixture model of a Newtonian fluid are effectively solved according to:

Conservation of Mass:

$$\frac{\partial \rho^{m}}{\partial t} + \nabla \cdot (\rho^{m} \mathbf{U}^{m}) = 0 \tag{44}$$

Conservation of Momentum:

$$\frac{\partial (\rho^{m} \mathbf{U}^{m})}{\partial t} + \nabla \cdot (\rho^{m} \mathbf{U}^{m} \otimes \mathbf{U}^{m}) = - \nabla p + \nabla \cdot \left[\mu^{m} (\nabla \mathbf{U}^{m}) + (\nabla \mathbf{U}^{m}) - \frac{2}{3} \mu^{m} \nabla \cdot \mathbf{U}^{m} \delta \right]$$
$$- \nabla \cdot \tau^{m''} + \rho^{m} \mathbf{g} + \mathbf{F}_{\sigma}$$
$$- \nabla \cdot \sum_{k=1}^{2} (\alpha^{k} \rho^{k} \mathbf{U}^{dr,k} \otimes \mathbf{U}^{dr,k})$$

(45)

Conservation of Energy:

$$\frac{\partial(\rho^m H^m)}{\partial t} + \nabla \cdot (\rho^m \mathbf{U}^m H^m) = \nabla \cdot (\lambda^m \, \nabla T^m) - \nabla \cdot \mathbf{q}_H^{m''} + \varsigma$$

$$- \nabla \cdot \sum_{k=1}^{2} (\alpha^k \rho^k \, \mathbf{U}^{dr,k} H^k)$$

(46)

In defining the above equations, both phases have been assumed to share the same pressure field: for this reason, the pressure in Eq.(45) is not the phase pressure.

The terms $\alpha^k \tau^{k''}$ and $\mathbf{q}_H^{k''}$ are connected to the turbulent nature of the flow, as already pointed out for the effective constitutive equations of the two-fluid model.

The quantity $\mathbf{U}^{dr,k}$ represents the drift velocity vector of the k-th phase, defined as the velocity of the disperse phase relative to that of the volume centre of the mixture, which can be expressed by $\mathbf{U}^{dr,k} = \mathbf{U}^k - \mathbf{U}^m$. As it can be seen, since the volume fraction α^k is present in Eq. (45) and (46), the model allows the phases to move at different velocities: in order to evaluate the phase velocities, an algebraic slip model is formulated.

The volume fraction of the the continuous phase can be computed by solving the individual phase equation (37); afterwards, the volume fraction of the dispersed phase can be evaluated from the $\sum_{k=1}^{2} \alpha^k = 1$.

In the absence of surface tension effects, the interfacial momentum source term $\mathbf{F}_\sigma$ and the interface energy source term ς can be neglected. In these circumstances, the governing equations are essentially the single-phase turbulent flow equations if the turbulent fluxes are retained or the single-phase laminar flow equations if the turbulent fluxes are ignored.

In the event where further simplification is introduced by assuming that the phase velocities are equivalent to each other, the mixture model reduces to the *homogeneous model*. This model is commonly adopted in most volume of fluid (VOF) computations (i.e., for free surface flows).

6   Generic form of the governing equation for the mixture and two-fluid models

By employing the general variable ϕ^m for the mixture model and ϕ^k for the two-fluid model, the generic forms of the governing equations can be written as:

Mixture model

$$\frac{\partial(\rho^m \phi^m)}{\partial t} + \nabla \cdot (\rho^m \mathbf{U}^m \otimes \phi^m) = \nabla \cdot [\Gamma_{\phi^m}(\nabla \mathbf{U}^m)] + S_{\phi^m}$$

(47)

Two-fluid model

$$\frac{\partial(\alpha^k \rho^k \phi^k)}{\partial t} + \nabla \cdot (\alpha^k \rho^k \mathbf{U}^k \otimes \phi^k) = \nabla \cdot \left[\alpha^k \Gamma_{\phi^k}^k (\nabla \mathbf{U}^k)\right] + S_{\phi^k}^k$$

(48)

7   Multi-phase models for gas-particle flows

In this Section, the techniques required for solving the motion of individual particles, moving through a gas phase, will be illustrated. Such systems are generally known as gas-particle flows. Gas-particle flows can be sub-divided into two sub-classes of flows, namely *gas-solid* and *gas-droplet* flows. The main difference between these two flows is that mass transfer does not occur in the former but occurs in the latter. An example of gas-solid flow is provided by cyclone separators while, regarding gas-droplet flows, we can cite the spray combustion of liquid fuel droplets within chemical combustors.

For the characterization of gas-particle flows, the concept of *mass loading* ratio is generally used:

$$ML = \frac{m_p}{m_g} \tag{49}$$

where m_p and m_g are the masses of particle and gas phases, respectively. When the ML ratio is small, the particles can be treated as passive contaminants.

7.1   Turbulent effects

Most gas-particle flows that are encountered in engineering systems are turbulent in nature. The interaction of particles with the turbulence of the gas phase is an important for gas-particle flows, since it leads to an apparently random spread of the particles throughout the flow field. The interaction between turbulent eddies and particulates is commonly referred to as *turbulent dispersion* because of the observed dispersive effect on particulates.

The effect of particle on the turbulence of the continuous phase is strictly linked to their size. In fact, while large particles tend to enhance turbulence due to the production of turbulent wakes, small particles are known to suppress the turbulence in the gas phase.

When small particulate is introduced in a turbulent flow, it will remain trapped inside an eddy for a certain time before the influence of another eddy. Since it is fair to assume that the eddy properties remain constant or uniform during the entire *eddy lifetime*[18], it is therefore common to suppose that a trapped particulate will experience a uniform velocity field during its residence time within an eddy.

The presence of particles can induce significant effects on the turbulence of the continuous phase. If the particle diameter is much smaller than the Kolmogorov scale, then turbulence modification is expected to be negligible, on condition that the mass loading ratio ML is sufficiently small: in fact, when the ML ratio is increased, global turbulence modifications may be induced. On the other hand, if the particle diameter is larger than the Kolmogorov scale, the particle affects the energy distribution of the surrounding fluid and, for sufficiently large ML ratio, the relative motion between particles and the carrier fluid leads to an extra dissipation of the turbulence energy.

Beyond the size of the particulate, there are other factors contributing to the turbulent dispersion, as the relative density between the particulate and the fluid, the fluctuating fluid velocity surrounding the particulate, the *particulate relaxation time*, the *eddy lifetime* and *particulate*

---

[18]The *eddy lifetime* is the maximum time for which a particulate can remain under the influence of a particular eddy.

Lagrangian time scale[19], and the cross-trajectory effect phenomenon[20].

Regarding the first factor, when the particulate density is much greater than that of the surrounding fluid, the inertia force at the fluid-particulate interface will damp the fluctuations in its velocity compared to the fluctuations of the surrounding fluid. This means that the fluctuating components of velocity for the particulate will be lower that those of the fluid. This reduction in the fluctuating velocity is known as the *inertia effect*, and it is characterized by a time scale called the *particulate relaxation time*.

The particulate relaxation time τ_p corresponds to the rate of response of particulate acceleration to the relative velocity between the particulate and the surrounding fluid, and can be expressed as:

$$\tau_p = \frac{4}{3}\frac{d_p^2}{\mu^g}\frac{\rho^p}{C_D}\frac{1}{\mathrm{Re}_p}, \qquad \underbrace{\mathrm{Re}_p = \frac{\rho^g\,|\mathbf{U}^g - \mathbf{U}^p|\,d_p}{\mu^g}}_{particulate\ Reynolds\ number} \tag{50}$$

where the particle Reynolds number Re_p is linked to the structure of the flow around the particle. In fact, for large Re_p, particles tend to generate turbulent wakes which will subsequently modify the turbulence of the carrier fluid. To quantify the nature of the kinetic equilibrium between the particles and the surrounding fluid, the *Stokes numbe*r can be introduced:

$$\mathrm{St} = \frac{\tau_p}{\tau_f} \tag{51}$$

where τ_f is the fluid integral scale. When $\mathrm{St} \ll 1$, the particles can be considered to be equilibrium with the carrier fluid while, for $\mathrm{St} \gg 1$, the inertia effect of particles becomes more prevalent and a significant momentum transfer from the particle to the fluid occurs.

7.2   Coupling between the phases

In a multi-phase flow, while the continuous flow always affects the motion of the disperse phase, the influence of the particulates of the carrier medium depends on the concentration of the disperse phase. In this sense, three forms of phase coupling can be recognized:

- One-way coupling. The fluid phase influences the disperse phase via aerodynamic drag and turbulence transfer, but the particulate phase does not affect the gas phase (i.e., the particles act as passive contaminants). In this way, the flow field of the continuous phase can be computed irrespective of the particle trajectories: the fluid velocities hence computed then can be introduced into the equations of motion of the particles, in order to determine their trajectories. This kind of coupling is an acceptable approximation for flows with low dispersed phase loadings for which the Stokes number is $\mathrm{St} \ll 1$.

- Two-way coupling. The inertia effects of particles become important and both the fluid phase and the disperse phase are influenced each other: the disperse phase reduces mean momentum and turbulent kinetic energy of the carrier medium. This case is encountered for large Stokes numbers ($\mathrm{St} \gg 1$). Two-way coupling requires the inclusion of particle source terms in the fluid momentum equations (the momentum sources could be due to

---

[19]The *particulate Lagrangian time scale* is roughly the time the particulate maintains its initial velocity before undergoing a turbulent collision and changing its velocity.

[20]The particulate does not remain trapped inside an eddy for the entire eddy lifetime but experiences a premature migration to another eddy. This happens when the minimum crossing time (i.e., the time taken to cross an eddy) is smaller than the eddy lifetime.

turbulent dispersion forces or drag). The particle source terms are generated for each particle as they are tracked through the flow.

- Four-way coupling. When the particle number density is sufficiently large, also the interactions among the particles are important; for their modeling, the Kinetic Theory of Gas is employed. The terminology "four-way" comes from the fact that if a particle A influences a particle B then, for the third law of dynamics, particle B must influence particle A.
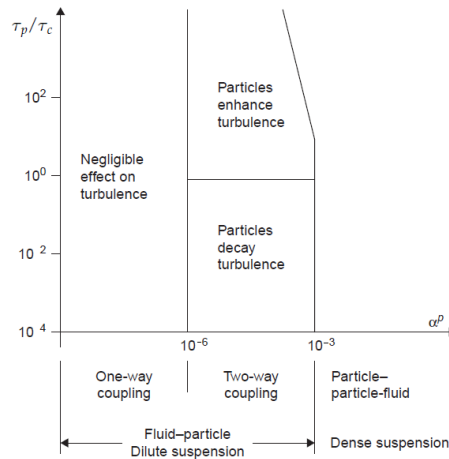
Figure 6: Classification of gas-liquid flows. From [10].

One useful way for determining which kind of coupling should be adopted is the use of the particle-turbulence modulation map, suggested by Elghobashi and illustrated in Fig.6. The Elghobashi's map reports the particle volume fraction α^p[21] along the x-axis, and the ratio between the particle relaxation time and the characteristics time of collisions, τ_p/τ_c, along the y-axis. The dilute regime is defined for $\tau_p/\tau_c \ll 1$ while the dense regime is for $\tau_p/\tau_c \gg 1$.

For dilute gas-particle flows, the fluid influence is the dominant effect since the time between two collisions is large enough for the motion of particles to be controlled by the fluid. Hence, a one-way coupling is sufficient for modeling the multi-phase flow. On the other hand, in dense gas-particle flows, the motion of particles is controlled by particle-particle collisions and interactions, because they do not have sufficient time to recover their own behaviour between two collisions. The motion of particles in a fluidized bed is one example of a dense gas-particle flow.

It is worth noting that no gas-particle flow can be completely dilute or dense, but rather one regime or the other may be more descriptive of the physical phenomenon in a specific case.

7.3   Eulerian and Lagrangian

As already said, the discrete particulates (small bubbles, particles or drops) co-flowing with a background fluid may be treated as either discrete or continuous phase. Therefore, two different approaches can be used for describing the particle phase, that is the *Lagrangian* and the *Eulerian* approach.

---

[21]The particle volume fraction α^p corresponds to the ratio of the volume V_p occupied by the particulate phase over the total volume V of the region of interest.

In the Lagrangian modality, which is sometimes referred to as *non-continuum* model, the motion of individual particles (or of a cloud of them) is tracked throughout the computational domain and the forces acting on them, which can alter the trajectory, are considered. Particulate trajectory is normally determined by solving the equation describing Newton's second law of motion through the instantaneous Eulerian fluid velocity field. In the Lagrangian approach, the reference frame employed for describing the particles' motion moves with the particles themselves. For dilute gas-particle applications, it is also possible to treat the particles as a continuous phase similar to the gas phase. In the Eulerian approach the reference frame is stationary and the particles pass through fixed differential control volumes. In this case, the particle motion is predicted by solving a set of continuum conservation equations which represent both gas and particle species (two-fluid model). For this reason, this approach is also known as *continuum* model.

In both cases, the background fluid is always solved in the Eulerian reference frame: therefore, it is common to speak of Eulerian-Lagrangian approach and Eulerian-Eulerian approach.

In Section 7.3.1 the Eulerian-Lagrangian approach is introduced, while in Section 7.3.2 the Eulerian-Eulerian modality is described.

7.3.1   Eulerian-Lagrangian framework

The Eulerian-Lagrangian approach resides in the effective coupling between a Eulerian field description for the solution of the surrounding fluid, and a Lagrangian scheme for determining the particulate trajectories within the continuous phase. The reference frame moves with the particulates, and the instantaneous position of a particle can be obtained as a function of the previous location and the elapsed time. The Eulerian part of this approach coincides with the solution of the continuous phase: in this case, the transport equations based on the two-fluid model can be adopted. The trajectories of the particulates are independently recovered later, through the use of convenient models.

The effects of inter-phase interactions in the continuous phase transport equations are modeled by summing the sources and sinks of representative trajectories. In the following Sections, the governing equations to resolve *dilute* gas-particle flows will be illustrated. As it can be appreciated from Fig. 6, the particle volume fraction for dilute gas-particle flows is much lower than unity, e.g. $\alpha^p < 10^{-3}$, and, therefore, a gas volume fraction close to unity can be assumed.

The trajectory equation   The trajectory of a particulate can be derived from the particulate momentum equation, which, in turn, can be deduced from Newton's second law of motion as

$$\underbrace{\rho^p U_p}_{m_p} \frac{D\mathbf{U}^p_{ins}}{Dt} = \underbrace{S_{V^p}}_{\sum \mathbf{F}} \tag{52}$$

where m_p is the particulate mass, ρ^p the particulate density, V_p the particulate volume and $\mathbf{U}^p_{ins} \equiv (u^p_{ins}, v^p_{ins}, w^p_{ins})$ the instantaneous particulate velocity. Equation (52) is an ordinary differential equation.

On the left-hand side of Eq.(52), the Lagrangian time derivative is essentially the material derivative of the particulate velocity, while on the right-hand side the source term S_{V^p} represents the sum of forces acting on the particulate, which can be of four kinds: (i) forces that act on the particulate due to its motion, (ii) forces that act on the particulate due to the motion of the surrounding fluid, (iii) forces that act on the particulate irrespective of the fact that it is moving or is immersed in a flowing fluid and (iv) forces that act on any object immersed in fluid irrespective of the motion. The forces that can act on the particulate are the following:

- *Drag force.* In most practical flows, the drag force is the most important force exerted on the particulate by the surrounding fluid. The drag force is induced by both the pressure distribution around the body (form drag) and by the viscous stress (skin friction). For spherical particles, the drag force can be formulated as:

$$\mathbf{F}_{drag} = \frac{\pi}{8} \rho^g d_p^2 C_D (\mathbf{U}_{ins}^g - \mathbf{U}_{ins}^p) \, |\mathbf{U}_{ins}^g - \mathbf{U}_{ins}^p| \tag{53}$$

where the superscript g refers to the continuous phase.

- *Virtual or added mass force.* It is originated from the difference in acceleration between the fluid and the particulate; it becomes dominant when there is a significant difference in the density of the fluid and the particulate:

$$\mathbf{F}_{Added} = 0.5 \, \rho^g U_p \frac{d(\mathbf{U}_{ins}^g - \mathbf{U}_{ins}^p)}{dt} \tag{54}$$

- *Basset force.* It addresses the temporal delay in boundary layer development as the relative velocity changes with time. It is also known as the *history term*, and is defined as:

$$\mathbf{F}_{Basset} = 6 \, d_p^2 \sqrt{\pi \rho^g \mu^g} \int\limits_0^t \frac{d(\mathbf{U}_{ins}^g - \mathbf{U}_{ins}^p)}{dt} \frac{dt'}{\sqrt{t - t'}} \tag{55}$$

- *Magnus force.* It arises when a rotating particulate is subjected to a non-rotating fluid, especially at high Reynolds number: a whirlpool of fluid is created around the particle and a force perpendicular to the line of motion is established:

$$\mathbf{F}_{Magnus} = \frac{\pi}{8} \, \rho^g d_p^3 \, \omega_p \, e_{ijk} \, n_{1,j} (\mathbf{U}_{ins}^g - \mathbf{U}_{ins}^p) \tag{56}$$

where $n_{1,j}$ is a unit vector in the direction of the angular momentum vector ω_p, while e_{ijk} is the order tensor ($e_{ijk} = 1$ if i, j and k are different and in cyclic order, $e_{ijk} = -1$ if i, j and k are different and in anti-cyclic order and $e_{ijk} = 0$ if any two indices are the same.

- *Lift force.* Small particles in a shear field experience a lift force perpendicular to the direction of flow. The shear lift originates from the inertia effects in the viscous flow around. The expression for the inertia shear lift was first obtained by Saffman:

$$\mathbf{F}_{Lift} = 1.615 \mu^{1/2} d_p^2 \, (\mathbf{U}_{ins}^g - \mathbf{U}_{ins}^p) \sqrt{\frac{\rho^g G}{\mu^g}} \tag{57}$$

where G is the magnitude of the velocity gradient in a shear flow.

- *Body force due to gravity.* The gravitational effects can be considered as:

$$\mathbf{F}_{Body} = \rho^p U_p \mathbf{g} \tag{58}$$

- *Bouyancy force.* It arises from the possible difference in densities between the fluid and the particulate:

$$\mathbf{F}_{Buoyancy} = -\rho^g U_p \mathbf{g} \tag{59}$$

- *Pressure gradient force.* It is the force required to accelerate the fluid which would occupy the particulate volume if the particulate were absent:

$$\mathbf{F}_{Pressure} = -\rho^g U_p \frac{D\mathbf{U}_{ins}^g}{Dt} \tag{60}$$

For the special case of dilute flow applications, especially when the particulate characteristic dimension is smaller than the Kolmogorov's length scale, the particulate-to-fluid density ratios are greater than 200 and the turbulent intensities are lower than 20%, the particulate can be assumed to be spherical in shape. Under these conditions, only the drag, gravity and buoyancy forces can be considered and, thus, Eq.(52) can be simplified as:

$$\frac{D\mathbf{U}_{ins}^p}{Dt} = \frac{1}{\tau_p} \left(\mathbf{U}_{ins}^g - \mathbf{U}_{ins}^p \right) + \left(1 - \frac{\rho^g}{\rho^p} \right) \mathbf{g} \tag{61}$$

where τ_p is the particle relaxation time.
The trajectory of the particle is recovered through the following relation:

$$\frac{D\mathbf{x}}{Dt} = \mathbf{U}_{ins}^p \tag{62}$$

As it results from Eq.(61), for the computation of the instantaneous velocity of the particulate, $\mathbf{U}_{ins}^p$, the instantaneous velocity of the continuous phase, $\mathbf{U}_{ins}^g$, is needed for determining the instantaneous source term. The instantaneous velocity of the gas phase is computed as:

$$\mathbf{U}_{ins}^g = \mathbf{U}^g + \mathbf{U}''^g \tag{63}$$

As it was discussed in the previous Sections, the solution of the Favre-averaged form of the transport equation for the continuous phase generally yields the mean values, and not the fluctuating ones.
In turbulent flows, if the fluctuating component of the fluid velocity is ignored while solving Eq.(61), the particulate dispersion due to turbulent velocity fluctuations will be neglected and only the convection of the particulates due to the mean flow will be taken into account. In this case, particles with the same physical properties and initial conditions (e.g., introduced in the same point of the domain) will cover the same trajectories. Such models, known as *deterministic models*, can only be applied to flows with very low turbulence levels.
For highly turbulent flows, in order to incorporate the dispersive effect of turbulent fluctuations on the particulate motion, it is necessary to employ *stochastic models*: in this way, particulates with the same physical properties and initial conditions do not necessary cover the same trajectory. For models based on the eddy lifetime concept, the eddy-particulate interaction is accounted by assigning a fluctuating velocity, U''^g, to a fluid eddy, which is assumed to remain constant during the lifetime of the eddy. The fluctuating velocity U''^g of an eddy is randomly sampled from a Probability Density Function (PDF); the particle turbulent dispersion can be correlated with the flow turbulent kinetic energy k as it follows:

$$U''^g = \zeta \sqrt{\frac{2}{3}k} \tag{64}$$

where ζ is a Gaussian random number. At the end of each time step, a new fluctuating fluid velocity is sampled from a new PDF.

By working with small time steps, for which the instantaneous fluid velocity and particle re-laxation time can be assumed to be constant, Eq.(61) can be analytically integrated in order to compute the time step velocity of the particulate as:

$$(\mathbf{U}_{ins}^p)^{n+1} = (\mathbf{U}_{ins}^p)^n \, e^{-\Delta T/\tau_p} + \left[\mathbf{U}_{ins}^g + \left(1 - \frac{\rho^g}{\rho^p} \right) \mathbf{g}\tau_p \right] \left(1 - e^{-\Delta T/\tau_p} \right) \tag{65}$$

where Δt is the time step. After having computed the velocity $\mathbf{U}_{ins}^p$, the position of the particulate can be determined by[22]:

$$(x^p)^{n+1} = (x^p)^n \, e^{-\Delta T/\tau_p} + 0.5 \, \Delta T \left[(\mathbf{U}_{ins}^p)^{n+1} + (\mathbf{U}_{ins}^p)^n \right] \tag{66}$$

In the Lagrangian framework, also heat and mass-transfer processes can be handled, from the corresponding conservation equations:

$$m_p c_p \frac{DT_p}{Dt} = S_{T_p} \tag{67}$$

$$\frac{Dm_p}{Dt} = S_{m_p} \tag{68}$$

where S_{T_p} and S_{m_p} denote the heat and mass transfer between the particulate and surrounding fluid, respectively.

Governing equations for the continuous phase   In the absence of heat transfer, the averaged form of the conservation equations for the continuous phase, based on the two-fluid model for a turbulent flow, are the following:

Conservation of Mass

$$\frac{\partial \rho^g}{\partial t} + \nabla \cdot (\rho^g \, \mathbf{U}^g) = 0 \tag{69}$$

Conservation of Momentum

$$\frac{\partial \rho^g U_i^g}{\partial t} + \frac{\partial}{\partial x_j}(\rho^g U_j^g U_i^g) = \frac{\partial}{\partial x_j} \left(\mu^g + \mu_T^g \right) \frac{\partial U_i^g}{\partial x_i} + S_{U_i^g} \tag{70}$$

In the momentum equations, the source or sink terms are given by:

$$S_{U_i^g} = -\frac{\partial p'^g}{\partial x_i} + \frac{\partial}{\partial x_j} \left(\mu^g + \mu_T^g \right) \frac{\partial U_j^g}{\partial x_i} + e S_{U^i}^p f \tag{71}$$

in which p'^g is the modified averaged pressure, defined as:

$$p'^g = p^g + \frac{2}{3} \rho^g k^g + \frac{2}{3} \left(\mu^g + \mu_T^g \right) \nabla \cdot \mathbf{U}^g \tag{72}$$

---

[22]In this case, a second order Crank-Nicolson scheme has been applied.

while $\mathbf{S}_U^p$ is the average momentum source or sink due to the motion of particles influencing the surrounding gas in a computational cell and, in the case of two-way coupling between the gas and particles, is expressed as:

$$\mathbf{S}_U^p = n \left\langle -m_p \left(\frac{D\mathbf{U}_{ins}^p}{Dt} - \mathbf{g} \right) \right\rangle \tag{73}$$

$\mathbf{U}_{ins}^p$ represents the instantaneous velocity of the particle, m_p the mass of the particle, n the mean number of particulates per unit volume, and the parentheses $\langle \rangle$ denotes the mean overall particulate trajectory realizations.

When the particle volume fractions are less than 10^{-6} (as in the very dilute particle regime) $\mathbf{S}_U^p$ can be set to zero and, therefore, the problem can be simplified to a one-way coupling.

7.3.2   Eulerian-Eulerian framework

The Eulerian-Eulerian approach solves the disperse phase as an ensemble of individual discrete phases flowing in the system. The Eulerian reference frame is stationary, and thus the fluid passes through fixed differential control volumes. The flow field of the continuous phase is obtained by solving the transport equations in a given coordinate system.

On the basis of the *two-fluid* model, the transport equations for the conservation of mass and momentum of the particle phase become:

Conservation of Mass

$$\frac{\partial \rho^{bp}}{\partial t} + \nabla \cdot (\rho^{bp}\, \mathbf{U}^p) = 0 \tag{74}$$

Conservation of Momentum

$$\frac{\partial \rho^{bp}\mathbf{U}^p}{\partial t} + \nabla \cdot (\rho^{bp}\mathbf{U}^p \otimes \mathbf{U}^p) = \nabla \cdot \tau^{p^{''}} + \mathbf{F}_G + \mathbf{F}_D + \mathbf{F}_{WM} \tag{75}$$

For dilute applications, it is common to take the bulk density ρ^{bp} equivalent to $\alpha^p \rho^p$, where α^p is the particle volume fraction.

The three additional source or sink terms in the momentum equation represent the gravity force $\mathbf{F}_G$, the drag force $\mathbf{F}_D$ and the wall-momentum transfer force $\mathbf{F}_{WM}$, which is due to particle-wall collision. The gravity force can be expressed as:

$$\mathbf{F}_G = \rho^{bp}\mathbf{g} \tag{76}$$

while the drag force[23]:

$$\mathbf{F}_D = \rho^{bp}\frac{f(\mathbf{U}^g - \mathbf{U}^p)}{\tau_p}, \quad \tau_p = \frac{\rho^p d_p^2}{18\mu^g} \tag{77}$$

The factor f appearing in Eq.(77) is a correction coefficient, which depends on the particulate Reynolds number.

---

[23]The drag force is due to the slip velocity between the gas and particle phase.

8   Interface capturing techniques

The methods for computing free surfaces and fluid interfaces between two immiscible fluids can be classified into two categories, the *surface methods* and the *volume methods*. The working principles of the two methods are illustrated in Fig. 7.

As explained in [10], the surface methods track the interface explicitly, by marking it with special marker points (particles) or by attaching it to a mesh surface which is then forced to move with the interface. In surface methods, the two-fluid approach is employed.

In the case of volume methods, both fluids are treated as single continuum. The fluids on either side of the interface are marked by either particles of negligible mass or an indicator function [10]. Marker particles can be spread over all fluid occupied regions and made to move with the fluid velocity. A cell containing an interface can be easily detected, since it contains markers but presents at least one neighboring cell with no markers. In order to get a well-defined interface, the number of particles must be sufficiently high. Therefore, although this method is enough simple, it suffers from a significant increase in required computer storage and time to move all the points to new locations [4].

For the methods based on a moving grid, the interface is treated as a sharp boundary whose motion is followed. On the contrary, for the methods based on fixed grids, the interface is moved through a fixed (Eulerian) grid. The advantage fixed-grid methods is that they can handle strong topological deformations of the interface such as merging and fragmentation.
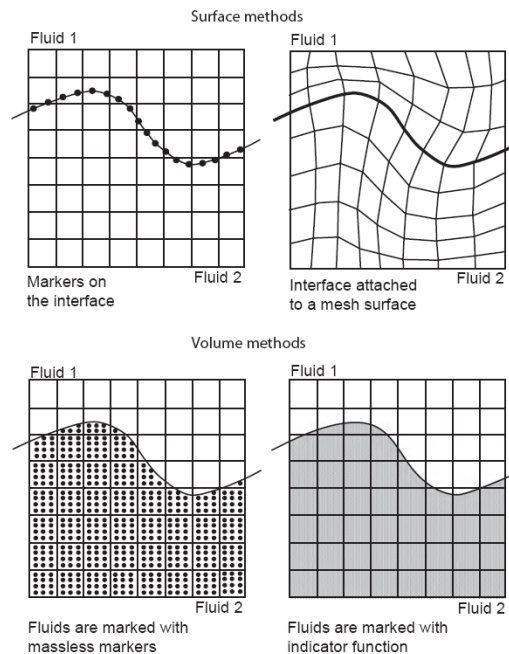

Figure 7: Methods for representing the behaviour of immiscible fluid separated by an interface. From [10].

8.1   Volume methods

Two approaches valid for fixed-grids are introduced, the *Level-set method* and the *Volume of fluid method* (VOF). The former has the advantage of its simplicity, but it can be not conservative, especially in the case of coarse grids. On the other hand, the conservation of mass is the

strong point of the VOF.

8.1.1   Level-set method

In the level-set method, the interface is defined by a level-set function ϕ, which is null at the interface, positive on one side and negative on the other. The ϕ function can be defined as the signed shortest distance of point x from the interface at time t, that is $\phi = \pm d(x, t)$. The level-set function is continuous on the domain and, therefore, can be differentiated everywhere.
Based on the calculated velocity field $\mathbf{U}^m$, the front evolves as a solution of a transport equation for ϕ:

$$\frac{\partial \phi}{\partial t} + \mathbf{U}^m \cdot \nabla \phi = S \tag{78}$$

which can be alternatively written in a conservative form:

$$\frac{\partial \phi}{\partial t} + \nabla \cdot (\mathbf{U}^m \phi) = \phi \nabla \cdot \mathbf{U}^m + S \tag{79}$$

In the above equations, $S = \dot{m} |\nabla \phi|$ and $\dot{m}$ is the mass flux of a phase at the interface divided by its density. S is null in the absence of any mass transfer due to phase change across the interface.
With the level-set formulation, the generic fluid property $b(\mathbf{x}, t)$ (density, viscosity, specific heat or thermal conductivity) is calculated by interpolating the corresponding values of the two phases, b_1 and b_2:

$$b(\mathbf{x}, t) = (1 - H_\varepsilon(\phi(\mathbf{x}, t)))b_1 + H_\varepsilon(\phi(\mathbf{x}, t))b_2 \tag{80}$$

in which H_ε is the Heaviside function, properly modified thus to be continuous.
As pointed out in [5], during the solution of the transport equation for ϕ, the level-set function does not remain a signed distance function at later times, which can lead to interface smearing, numerical diffusion and difficulties in preserving the mass conservation. Therefore, in order to fix these problems, some re-initialization techniques are employed: ϕ is reinitialized regularly in the vicinity of $\phi = 0$, so that $|\nabla \phi| = 1$.
For the discretization of the advection term of Eq. (79) a non-diffusive differencing scheme must be adopted. Moreover, if the mesh is not sufficiently fine, it would be useful to adopt higher-order schemes so that the sharp shape of the interface is maintained and its smearing avoided.

8.1.2   Volume of fluid (VOF) model

The volume of fluid (VOF) model is a interface-capturing technique applied to a fixed Eulerian mesh. In this method, the motion of the interface is not tracked directly, but the volume fraction of one phase is evolved in time: the interface is then reconstructed according to the values assumed by the volume fraction itself.
The VOF can be applied to immiscible fluids with clearly defined interface, when the shape of the interface is of interest. This method is inappropriate if bubbles are small compared to the control volume (e.g., bubble columns). Moreover, it can not resolve details of the interface smaller than the mesh size.
In the VOF model, a single set of momentum equations is shared by the fluids (*Mixture model* formulation), and the volume fraction of one fluid is tracked throughout the domain.

The VOF formulation relies on the fact that the different phases are not interpenetrating. The method assumes that each control volume contains only one phase, or the interface between phases. For distinguishing the two fluids, a scalar indicator function, F, named *Colour function*, is employed. Let us suppose that this function is defined according to the phase i (usually the liquid phase). Then it can be said that the colour function corresponds to the volume fraction of the phase i within the volume V. Conventionally, the indicator function is denoted as:

$$F = \lim_{V \to \infty} \frac{1}{V} \int \int \int \chi^k(x, y, z, t) \, dV = \left\langle \chi^k \right\rangle \tag{81}$$

From this definition it can be easily deduced that the colour function is defined between zero and unity. A value of one indicates the presence of the phase i, while a value of zero indicates that the cell is occupied by the second fluid. If a cell contains the interface, then F assumes a value intermediate between 0 and 1, which corresponds to the proportion of phase i present in the control volume. From this, it can be inferred that F is a discontinuous function.

Besides the identification of the cells containing a boundary, the F function can be even used to define the position of the interface. In fact, the gradient of F can be used to identify the direction normal to the interface (since F is a step function, spacial care must be exercised in the definition of its derivatives). When the normal direction is known, then a line cutting the cell can be traced, which approximates the interface.

Since in the VOF method a *Mixture formulation* is used, a single set of equations can be written for the two-phase system. The density and the dynamic viscosity can be calculated through the indicator function, F:

$$\rho(F) = \rho_l F + \rho_g (1 - F) \tag{82}$$
$$\mu(F) = \mu_l F + \mu_g (1 - F) \tag{83}$$

To track the evolution of the interface, an advection equation for the volume fraction F need to be solved[24]:

$$\frac{\partial F}{\partial t} + \nabla \cdot (F \mathbf{U}) = 0 \tag{84}$$

in which $\mathbf{U}$ is the velocity of the fluid. Equation (84) says that the volume fraction advects with the velocity computed in the flow field. It is worth noting that the advection of the volume fraction corresponds to the computation of a mass flux through a cell face: the shapes of the interfaces and the advection of the volume fraction should be exactly calculated to conserve the mass of each phase and to keep a sharp definition of the interfaces.

VOF algorithms consists of three major parts [2]:

- an *interface reconstruction* method, which provides an explicit description of the interface in each cell based on void fractions at the current time step;

- an *advection algorithm*, which calculates the distribution of *F* at the next time step by solving an advection equation and using the present reconstructed interface and velocity field;

- a *surface tension model*, which takes into account the surface tension effects at the interface.

---

[24]This equation is valid under the assumption of incompressible flow.

The success of a VOF method is strongly connected to the numerical scheme used for the advection of the F. A first order upwind scheme introduces an artificial diffusion and smears the interface (the interface is not located in correspondence of only one cell but its extension increases with time). The numerical diffusion can be overcome by employing higher order schemes: however, a second order scheme can be unstable and induce unrealistic oscillations of the interface profiles.

In the years, several techniques have been proposed for reconstructing the interface, which can be basically grouped into two categories, the piecewise constant approximation and the piecewise linear approximation. Belong to the former group, the Simple Line Interface Calculation (SLIC) algorithm of Noh and Woodward (1976) and the Donor-acceptor method of Hirt and Nichols (1981) [4]. The piecewise linear approximation group includes the PLIC method of Youngs (1982), and its improved versions, named FLAIR, LVIRA, FLVIRA. Some of the aforementioned methods are summarized in Fig. 10.
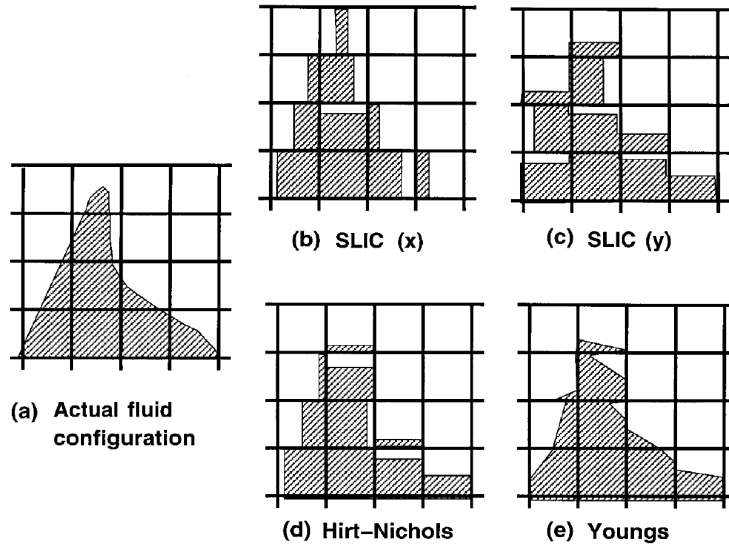

Figure 8: Some methods for interface reconstruction. From [8].

In the SLIC method, the reconstructed interface is constituted by a sequence of line segments aligned with the grid. The interface can assume different configurations for each sweep direction (x and y axes).

The Donor-Acceptor Method uses information about F downstream as well as upstream of a flux boundary. The donor cell is a control volume which provides the fluid, while the acceptor cell is the control volume that receives the fluid. Let us consider the case of a uniform 2D structured grid of size δx and δy. The total flux of fluid and void volume crossing the face of a computational cell, per unit cross sectional area and in the time δt, is equal to $V = U\delta t$, where U is the normal velocity at the face. The sign of U determines the donor and acceptor cells: if U is positive, the donor cell is on the left of the acceptor cell. The amount of F fluxed across the cell face in one time step is:

$$\delta F \delta y = \min \left[F_{AD} \left| V \right| \delta y + CF, \ F_D \delta x \delta y \right] \tag{85}$$

$$CF = \max \left[(1 - F_{AD}) \left| V \right| \delta y - (1 - F_D)\delta x \delta y, \ 0 \right] \tag{86}$$

In the above equations, D and A represent a donor and an acceptor cell, respectively, while the subscript AD refers to either A or D, depending on the orientation of the interface relative to

the direction of flow: the acceptor cell is used when the interface is advected mostly normal to itself [6].

The min function in Eq. (85) ensures that the amount of fluid transferred to the acceptor cell, $F_{AD}\,|V|\,\delta y + CF$, is always lower than the amount of fluid available in the donor cell, $F_D \delta x \delta y$. The term CF represents an additional flux: the max function guarantees that the amount of void, $(1 - F_{AD})\,|V|$, to be fluxed is not higher than that existing in the donor cell, $(1 - F_D)\delta x \delta y$. After having determined the amount of F advected, the volume fraction in the donor cell decreases by the same amount while that in the acceptor cell increases by the same amount.

In order to clarify the ideas, please refer to Fig. 9, which refers to a case where $AD = A$ (the donor cell is on the left). In this case, the quantity of fluid which must be transfered from D to A is higher to that leaving the A cell, $F_A U \delta t \delta y$. The extra quantity of fluid to be fluxed to A corresponds to CF. For the case considered, the void leaving the A cell is higher than the amount of void transferred from D to A.

In essence, the VOF method by Hirt and Nichols uses first-order upwind and downwind fluxes combined in such a way as to ensure stability of the numerical calculation and at the same time as to minimize diffusion [5].
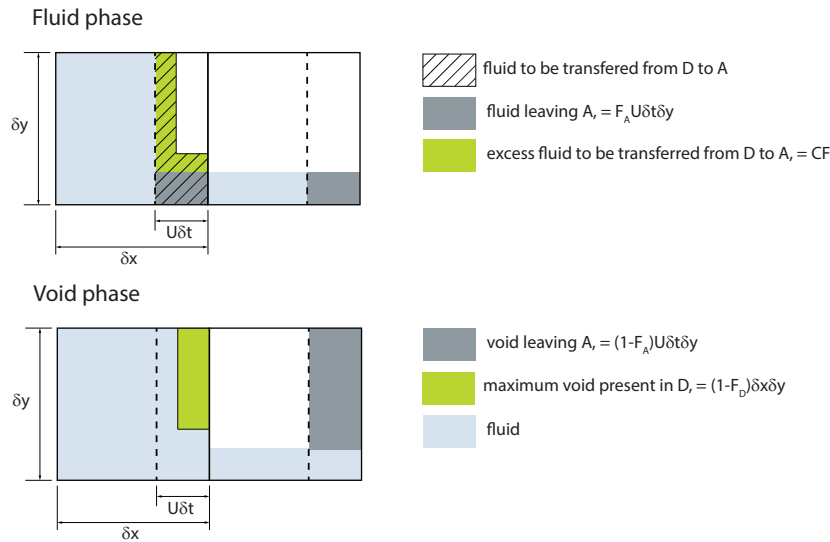

Figure 9: Donor-acceptor method for the case $AD = A$. The donor cell is on the left.

Youngs' PLIC method uses a more accurate interface reconstruction than that the Hirt-Nichols' one, since it fits the interface through oblique lines or piecewise linear segments. In this case, within each cell the interface can be defined as a straight line expressed by the equation:

$$n^x x + n^y y = \beta \tag{87}$$

being $\vec{n} = (n^x, n^y)$ the normal vector to the interface, and β a constant. Firstly, the normal vector $\vec{n}$ is computed, usually starting from the gradient of the volume fraction of each control volume (the interface will be perpendicular to $\vec{n}$). Then, the correct placement of the interface line has to be determined, by calculating the value of β: basically, the fraction of the cell area cut by the linear segment and occupied by the reference phase must equal the volume fraction. In Fig. 10 the possible polygon areas that can be realized with the PLIC algorithm, within a
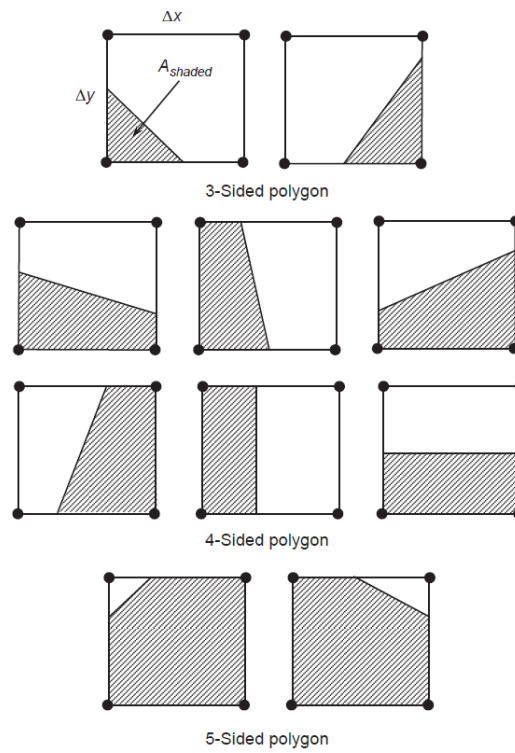
Figure 10: Possible candidates of interface reconstruction with the PLIC algorithm in a structured rectangular mesh cell. From [10].

rectangular mesh cell, are illustrated.

It is worth noting that, in the PLIC method, the interface is not required to be a continuous chain of segments. The method of Youngs was shown to be very robust and efficient, but only of first-order accuracy [2].

9   Multi-phase modeling in ANSYS CFX

Two distinct multiphase flow models are available in ANSYS CFX, an Eulerian-Eulerian multiphase model and a Lagrangian Particle Tracking multiphase model.

Two distinct models are available for Eulerian-Eulerian multiphase flow: the *homogeneous* model and the inter-fluid transfer or *inhomogeneous model*. The former is applicable when all the fluids share the same velocity fields, as well as other fields (e.g., temperature, turbulence...), the latter should be used when each fluid possesses its own flow field and the fluids interact via interphase transfer terms. Therefore, one solution field for each separate phase exists.

For the *inhomogeneous model*, three different sub-models are available, that is the *particle model*, the *mixture model* and the *free surface model*.

The particle model can be applied when one of the phases is continuous and the other is dispersed (e.g., gas bubbles in a liquid, liquid droplets in a gas or in immiscible liquid, solid particles in a gas or in a liquid). In this model, the particles or droplets are assumed to be spherical.

The mixture model treats both phases symmetrically and requires both phases to be continuous. It can be used to model, for example, Churn flows.

The free surface model is applicable to free surface flows. In this case, in presence of entrainment of one phase inside another, also the mixture model may be used.

For the inhomogeneous model, the constraint on the volume fractions α^k is combined with the phasic continuity equations thus to obtain a transported volume conservation equation.

For further details on the Eulerian model, please refer to *Multiphase Flow Theory* in the *CFX-Solver Theory Guide* and to *Multiphase Flow Modeling* in the *CFX-Solver Modeling Guide*.

The Particle Transport model is capable of modeling dispersed phases (solid particles, droplet, or bubble) which are discretely distributed in a continuous phase. Each phase is computed from separated simulations, and source terms are introduced to account for the effects of the particles on the continuous phase. Examples of this kind of motion are provided by the motion of water droplets, generated from a liquid sprays in a cooling tower, in air, the motion of solid particles in air in the case of pneumatic transport of solids, and the transport of airborne particulates.

For further details on the Lagrangian model, please refer to *Particle Transport Theory* in the *CFX-Solver Theory Guide* and to *Particle Transport Modeling* in the *CFX-Solver Modeling Guide*.

Nomenclature

C_D Drag coefficient
D Tube diameter [m]
F_σ Interfacial momentum source term
G Mass flux $\left[\text{kg/m}^2 \cdot \text{s}\right]$
G Magnitude of the velocity gradient in a stress flow
H Total enthalpy
M Number of phases
ML Mass loading ratio
N Number of samples, see Eq.(4)
Re   Reynolds number
St   Stokes number
T Time
T Temperature, see Eq.(**??**)
U   Velocity
V Volume

d_p Particulate diameter
f Correction factor, see Eq.(77)
j Volumetric flux $\left[\text{m}^3/\text{m}^2 \cdot \text{s}\right]$
m Mass
$\dot{m}$ Mass flow rate
n Mean number of particulates per unit volume
p Pressure
q Exchanged heat
t, t' Time
x Spatial coordinate
y Spatial coordinate
z Spatial coordinate

α Local volume fraction
Γ^k Interfacial mass source term for phase k
Γ'^k Interfacial mass source term for phase k (after Favre and time averaging)
δ Kronecker delta
λ Thermal conductivity
μ Dynamic viscosity
Π^k Interfacial energy source term for phase k
Π'^k Interfacial energy source term for phase k (after Favre and time averaging)
ρ Density
ς Interfacial energy source term
τ Extra stress tensor
τ_f Fluid integral scale
τ_p Particulate relaxation time
ϕ Generic transport variable
$\phi^{“}$ Fluctuating component of $\langle \phi \rangle$
χ Phase indicator function
ψ Generic transport variable
$\psi^{“}$ Fluctuating component of $\langle \psi \rangle$

ω Angular momentum vector
Ω^k Interfacial momentum source term for phase k
Ω'^k Interfacial momentum source term for phase k (after Favre and time averaging)

Superscripts

bp Bulk
d Drift
g Gas
int Interphase
k Phase
m Mmxture
p Particulate

Subcripts

D Drag
E Ensemble average
G Gravity
p Particulate
k Phase
SG Superficial gas
SL Superfical liquid
V Space average
WM Wall-momentum transfer
f Fluid phase
j Phase
ins Instantaneous

References

[1] G.P. Celata, M. Cumo, D. Dossevi, R.T.M. Jilisen, S.K. Saha, and G. Zummo. Flow pattern analysis of flow boiling inside a microtube. In *XXVIII Congresso sulla Trasmissione del Calore, Brescia, 21-23 Giugno 2010*.

[2] D. Gerlach, G. Tomar, G. Biswas, and F. Durst. Comparison of volume-of-fluid methods for surface tension-dominant two-phase flows. *International Journal of Heat and Mass Transfer*, 49:740–754, 2006.

[3] A.J. Ghajar. Non-boiling heat transfer in gas-liquid flow in pipes - a tutorial. *J. of the Braz. Soc. of Mech. Sci. & Eng.*, 27(1):46–73, 2005.

[4] C.W. Hirt and B.D. Nichols. Volume of fluid (VOF) method for the dynamics of free boundaries. *Journal of Computational Physics*, 39:201–225, 1981.

[5] M. Ishii and T. Hibiki. *Thermo-fluid dynamics of two-phase flow*. 2006.

[6] B.D. Nichols, C.W. Hirt, and R.S. Hotchkiss. SOLA-VOF: a solution algorithm for transient fluid flow with multiple free boundaries. 1980. www.ewp.rpi.edu/hartford/ ernesto/F2012/CFD/Readings/SOLA-VOF-1980-P1.pdf.

[7] P. Poesio and G. Sotgia. Multiphase oil-water-gas flow: a research field worthy of further and deeper investigation. In Società Esculapio Editrice, editor, *UIT XXVII Congresso sulla Trasmissione del Calore*, pages 3–16, 2009.

[8] F.S. Qi, G.H. Yeoh, S.C.P. Cheung, J.Y. Tu, E. Krepper, and D. Lucas. Volume-tracking methods for interfacial flow calculations. *International Journal for Numerical Methods in Fluids*, 24:671–691, 1997.

[9] F.S. Qi, G.H. Yeoh, S.C.P. Cheung, J.Y. Tu, E. Krepper, and D. Lucas. Classification of bubbles in vertical gas-liquid flow: Part 1 - an analysis of experimental data. *International Journal of Multiphase Flow*, 39:121–134, 2012.

[10] G.H. Yeoh and J. Tu. *Computational techniques for Multiphase Flows*. 2010.